Redox FTIR difference spectroscopy using caged electrons reveals contributions of carboxyl groups to the catalytic mechanism of heme-copper oxidases. FEBS Lett

ARTICLE *in* FEBS LETTERS · DECEMBER 1996

Impact Factor: 3.17 · DOI: 10.1016/S0014-5793(96)01174-X · Source: PubMed

Redox FTIR difference spectroscopy using caged electrons reveals contributions of carboxyl groups to the catalytic mechanism of haem-copper oxidases

Mathias Lübben*, Klaus Gerwert

Lehrstuhl für Biophysik, Ruhr-Universität Bochum, Universitätsstr. 150, 44780 Bochum, Germany

Received 16 September 1996

Abstract Redox spectra of the haem-copper oxidases cytochrome aa_3 of *Rhodobacter sphaeroides* and cytochrome bo_3 of *Escherichia coli* were recorded in the visible and infrared spectral regions. The reduction of oxidases was initiated after light activation of the 'caged electron' donor riboflavin. Infrared redox difference spectra exhibit absorbance changes in the amide I region, which are indicative of very small redox-linked conformational movements in the polypeptide backbone. A reproducible redox-dependent pattern of positive and negative absorption changes is found in the carbonyl region (1680–1750 cm^{-1}). The carbonyl bands shift to lower frequencies due to isotope exchange of the solvent H_2O to D_2O. This common feature of cytochrome *c* and quinol oxidases indicates that at least (i) one redox-sensitive carboxyl group is in the protonated state in the oxidized form and (ii) one carboxylic acid is involved at a catalytic step – presumably in proton translocation – of haem-copper oxidases.

Key words: Cytochrome bo_3; Cytochrome aa_3; Haem-copper oxidase; FTIR; Caged electron

1. Introduction

Haem-copper oxidases belong to the superfamily [1,2] of cytochrome oxidases, which use either cytochrome *c* or ubiquinol as substrates. They are found in all groups of organisms, in eukaryotes and eubacteria [3] as well in the archaea [4]. Cytochrome oxidases act as terminal catalysts of the respiratory chain and transfer substrate electrons to molecular oxygen resulting in the production of water. The enzymatic activity is coupled to the generation of an electrochemical potential of protons across the cytoplasmic or organellar membranes. A proton gradient is formed by two different mechanisms: (i) scalar – by proton uptake at the oxygen binding side of the membrane; and (ii) vectorial – by direct translocation of protons across the membrane. It has been proposed that protons are conducted through membrane-spanning hydrogen-bonded network(s) anchored by polar and/or charged amino acid residues [5,6]. A number of residues which could take part in networks have been suggested for the putative proton channel from the recently solved structure of the cytochrome oxidase of *Paracoccus denitrificans* [7]. This scheme of proton channel forming residues differs in some aspects from a proposal supported by the crystal structure data of the mitochondrial cytochrome *c* oxidase [8].

Data from X-ray crystallography provide the structural base for the prediction of functional features. Nevertheless, infrared difference spectroscopy permits a more detailed insight into certain regions of proteins, which finally results in a model with higher structural resolution. For haem-copper oxidases this would hold especially for the spatial orientations of amino acid side chains that (i) are metal ligands or are located in proximity of the binuclear haem-copper reaction centre and (ii) are involved in a hydrogen-bonded network within the proton channel(s). In addition, the function of proteins can be non-invasively investigated with FTIR by means of atomic bonds of prosthetic groups or of amino acids as endogenous probes. Hence, the primary aspects of the molecular mechanism of haem copper oxidase can be addressed, i.e. (i) the process of electron transfer-linked oxygen reduction plus water formation and (ii) the mechanism of transmembrane proton translocation.

The observation of catalytic mechanisms by FTIR is based on the measurement of absorbance differences after the initiation of an enzymatic reaction. In the case of the cytochrome oxidase the uptake of substrate electrons is the first step of catalytic action. This requirement would be optimally fulfilled with a caged compound, which after light induction releases electrons into the oxidized protein. The study describes the use of a flavin compound (='caged electron') in order to investigate the mechanism of two representatives of the haem-copper oxidase superfamily, a cytochrome *c* oxidase (cytochrome aa_3 of *Rhodobacter sphaeroides*) and a ubiquinol oxidase (cytochrome bo_3 of *Escherichia coli*).

2. Materials and methods

2.1. Sample preparation

The four-subunit cytochrome bo_3 of *E. coli* was prepared after tagging the C-terminus of subunit IV of the complex with oligohistidine by means of an immobilized metal affinity column (to be published elsewhere). The cytochrome aa_3 of *R. sphaeroides* (two subunit version 'P2') was prepared as described [9] and was kindly provided by Antony Warne. The oxidase samples were diluted with a buffer containing 20 mM Tris-Cl, 0.3% decylmaltoside, pH 8.0 and were concentrated by spin filtration with Centricon 30 plus Microcon 30 assemblies (Amicon) to 0.4–0.6 mM. Solvent isotope exchange from H_2O to D_2O was performed by two cycles of 20-fold dilution of the aqueous sample with buffer made up in D_2O after lyophilisation and subsequent concentration with Microcon 30.

4–8 μl of the air-oxidized protein solution (about 0.3 mM) was mixed with 0.8 μl of a solution containing 0.5 mM of riboflavin and 100 mM EDTA. The mixture was added on a greased CaF_2 plate and exposed for 3 min in a vacuum desiccator connected with a water aspirator pump. The mixture was homogenized by a plastic spatula and squeezed by means of a second CaF_2 plate. The sandwich was inserted into a workshop-made cuvette frame and stored for several hours in the dark at 4°C before mounting into the spectrometer.

2.2. Spectroscopy

Infrared spectra between 1800 and 1000 cm^{-1} at 4 cm^{-1} spectral

*Corresponding author. Fax: (49) (234) 709-4238.
E-mail: luebben@bph.ruhr-uni-bochum.de

PII S0014-5793(96)01174-X

resolution were taken on a Bruker IFS66v spectrometer positioned on a vibration-decoupled table (Newport). In order to minimize the absorption of H_2O vapour the infrared beam path of the spectrometer was evacuated to a residual air pressure of < 5 mbar, except for the workshop-made sample chamber, which was purged with dry and clean air (Balston purge gas generator). After equilibration at 25°C, a reference infrared spectrum of the air-oxidized sample was taken by co-addition of 400 interferograms at a rate of 10 scans/s. The photoreduction was initiated by laser light at 308 nm from an excimer laser (LPX 240i, Lambda Physik) with pulse energy of 130–140 mJ. The incident laser light intensity at the sample position was estimated to 20 mJ per pulse. After application of 20 laser flashes with 1 Hz repetition rate, infrared spectra of the photoreduced oxidase were taken by accumulating 400 scans. This program was repeated as long as subsequently recorded infrared spectra became identical (usually 5 times). Co-added interferograms were manipulated by zero filling with a factor of 2 and Fourier-transformed using Mertz phase-correction and the Blackman-Harris 3-term apodization function. Reduced-*minus*-oxidised FTIR difference spectra were calculated by subtraction of the spectra of photoreduced and air-oxidized states.

Before and after the photoreduction carried out in situ in the infrared spectrometer, optical spectra of oxidized and reduced states were recorded on a dispersive Hitachi 220A spectrophotometer equipped with a workshop-made IR cuvette holder in the range of 650 and 400 nm.

The photoreduction of cytochrome bo_3 in the membrane-bound and purified state was measured in free solution after irradiation with a 150 W lamp (Xenophot HLX) via light guides fitted to the cuvette. After irradiation intervals of 5 s, reduced-oxidized difference spectra were recorded with an Aminco DW 2 spectrophotometer at room temperature.

3. Results and discussion

3.1. Riboflavin acts as a caged electron

In earlier studies using optical spectroscopy, riboflavin has been described as a photoinducible reductant of cytochrome *c* and cytochrome *c* oxidase [10,11].

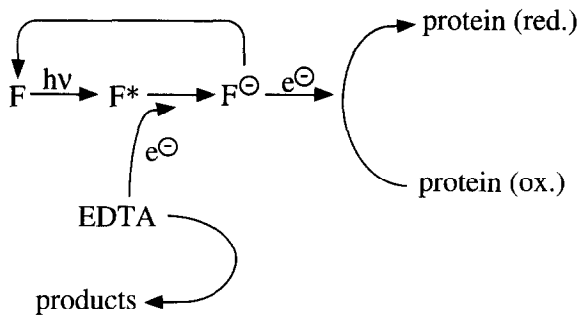

Fig. 1. Reaction scheme of the photoreduction mechanism with the caged electron compound riboflavin (F), simplified for the sake of clarity. The asterisk (*) represents the photoactivated state and the '–' sign indicates the uptake of an electron without further specification of the half or fully reduced states of riboflavin. More details about the reaction mechanism of flavins is given in [12,23].

The mechanism of cytochrome oxidase reduction initiated by light-induced release of electrons (caged electrons) is discussed in detail in [12] and is schematically outlined in Fig. 1. Light absorption leads to formation of an activated state F* with a redox potential sufficient for extraction of electrons from the 'sacrificial' electron donor EDTA. The reduced form (for simplification symbolized as F^-) could donate electrons directly to the protein. As long as EDTA is present in excess, the reduced form of riboflavin is continuously regenerated.

The potency of riboflavin to photoreduce also the quinol

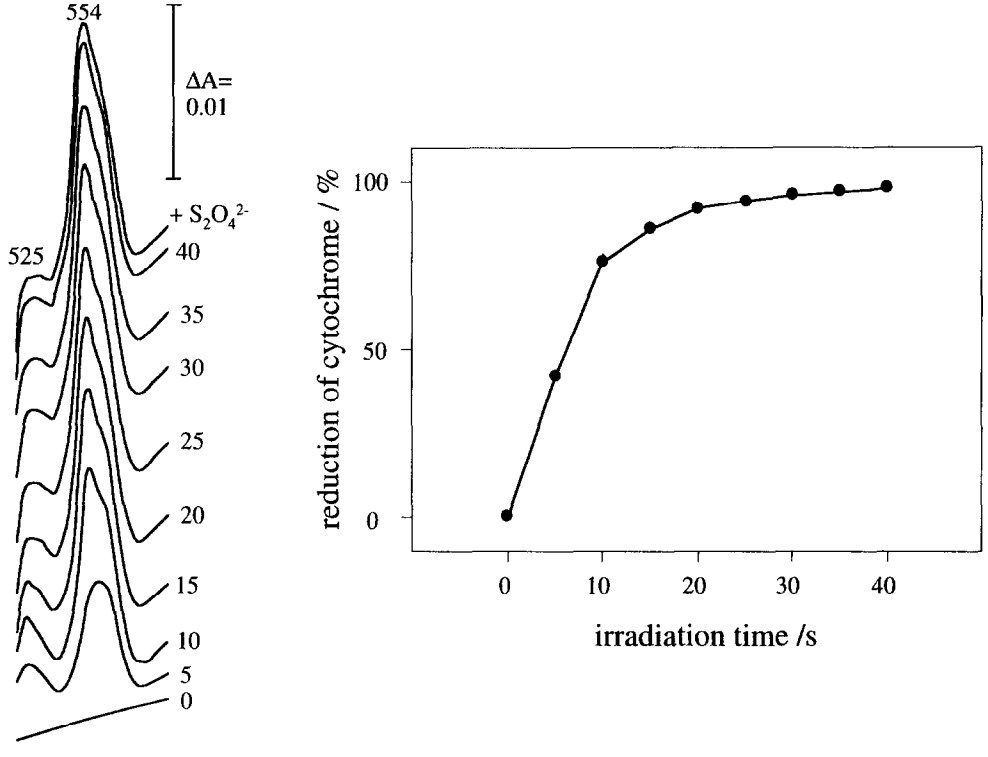

Fig. 2. Photoreduction of a 2 μM solution of purified cytochrome bo_3 in 50 mM potassium phosphate, pH 7.0, 5 mM EDTA, 0.1% Triton X-100, 0.2 mM KCN. Redox difference spectra were taken after illumination as described in Section 2. For clarity the spectra are plotted with offsets (left). After 40 s, addition of dithionite did not further change the spectra, indicating completion of the reaction. The time course of the photoreduction is plotted to the right. The degree of reduction is defined by the difference in the absorption spectra, assuming the one between 0 and 40 s of illumination as 100%.

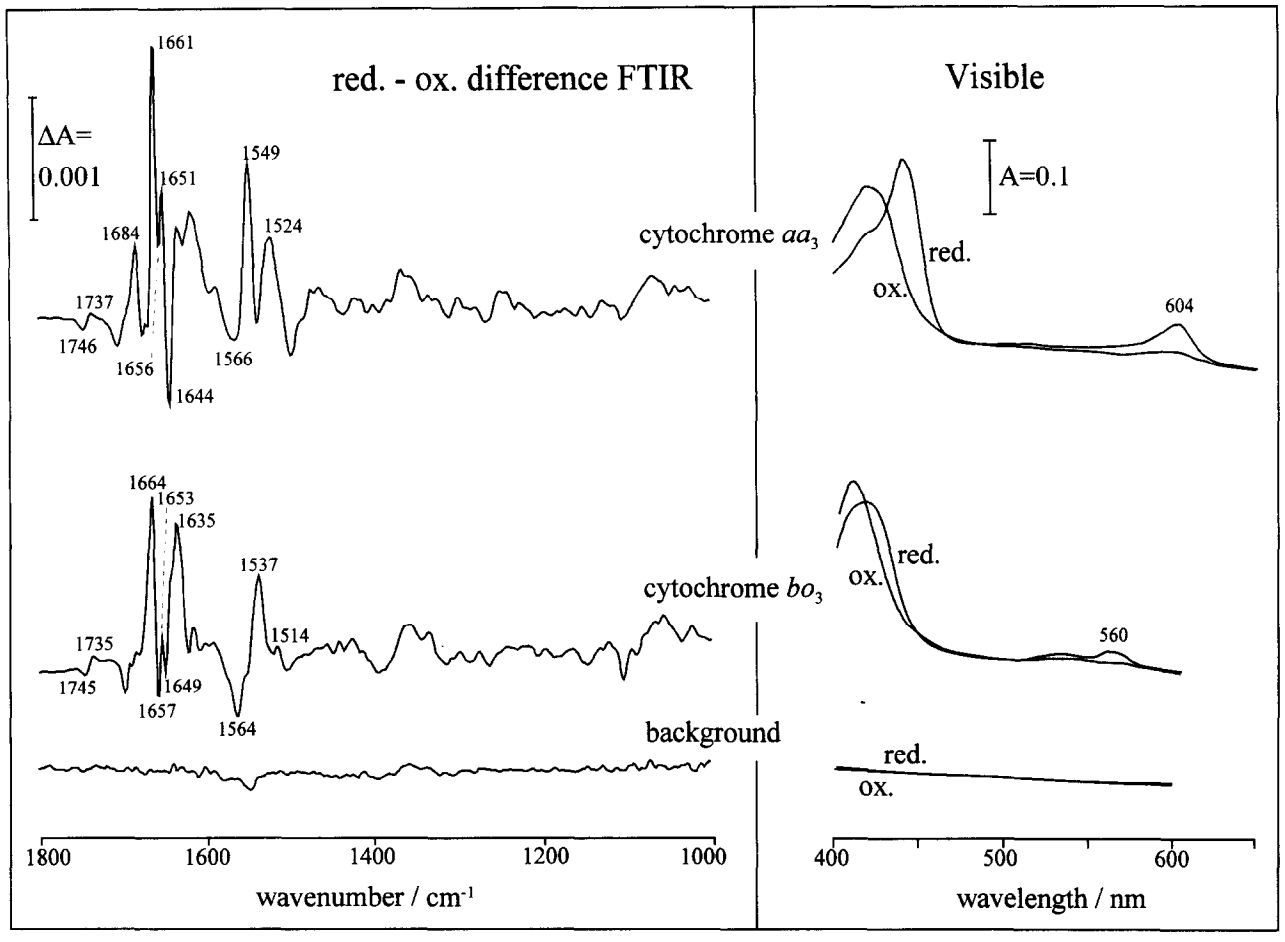

Fig. 3. Redox FTIR absorbance difference spectra (left) and absolute visible absorbance spectra (right) of the cytochrome *c* oxidase cytochrome aa_3 of *Rhodobacter sphaeroides* (top) and of the ubiquinol oxidase cytochrome bo_3 of *Escherichia coli* (middle). The background spectra (bottom) were taken from a sample containing the reagent without protein.

oxidase cytochrome bo_3 from *Escherichia coli* was assessed. Fig. 2 shows the visible absorbance difference spectra (left) and the time course (right) of cytochrome bo_3 reduction during steady-state illumination with a halogen lamp. The molar ratio of cytochrome oxidase to riboflavin was 50:1. In order to prevent reoxidation of the protein due to the high concentration of dissolved oxygen, 0.2 mM KCN was added to the sample. Under these conditions, the oxidase could be photoreduced completely, it reached about 70% after 10 s of irradiation (Fig. 2, right). In the spectral range of 520–600 nm, only the chromophores of the protein significantly contribute to the total absorbance.

3.2. Redox-FTIR of haem-copper cytochrome oxidase

The absorbance changes of reduced and oxidized forms of haem-copper oxidases in the infrared spectral region are very small as compared with the total absorbance of the samples. If the absorbance changes are in the order of 0.1–0.2%, sensitive recording of infrared difference signals requests the redox transition to take place in situ, i.e. without moving the sample cuvette. Therefore, the principle of riboflavin photochemistry has been further developed for studying the effects of light induced cytochrome oxidase reduction monitored by Fourier-transform infrared spectroscopy. Reduced-*minus*-oxidized spectra of cytochrome bo_3 of *E. coli* and of cytochrome aa_3 of *R. sphaeroides* are shown in Fig. 3 (left). The spectra evolve after applying incident ultraviolet laser light for up to 100 flashes. Although the oxidized form of riboflavin has an absorbance minimum at 308 nm, light activation of the compound is very efficient due to the high light intensity of the excimer laser. The applied intensities do not damage the samples, since in a control experiment continuous irradiation for 5 min at 100–150 W with a halogen lamp results in similar spectra (data not shown). Also optical spectra, which were taken before and after the laser irradiation, indicate the integrity of samples (Fig. 3, right): the absolute electronic absorbance spectra of cytochrome bo_3 and cytochrome aa_3 exhibit the band patterns typical of oxidized and reduced haems bound to their native apoproteins. The latter spectra also demonstrate that the photoreduction of oxidases is completed.

Aqueous biological samples have to be applied as very thin layers between the two CaF_2 plates (usually less than 20 μm thick) because of the strong absorbance of water in the spectral region of interest. In order to obtain a reasonable absorbance of the sample, the oxidases must be concentrated to the limit of solubility. In order to keep the absorbance changes from the caged compound alone as low as possible, the molar ratio of cytochrome oxidase to riboflavin was at least 5. The difference spectrum of the caged compound in buffer without protein is shown in Fig. 3 (bottom). The contribution of riboflavin and the photolytic products of the electron donor EDTA (Fig. 1) to redox FTIR difference and optical absorb-

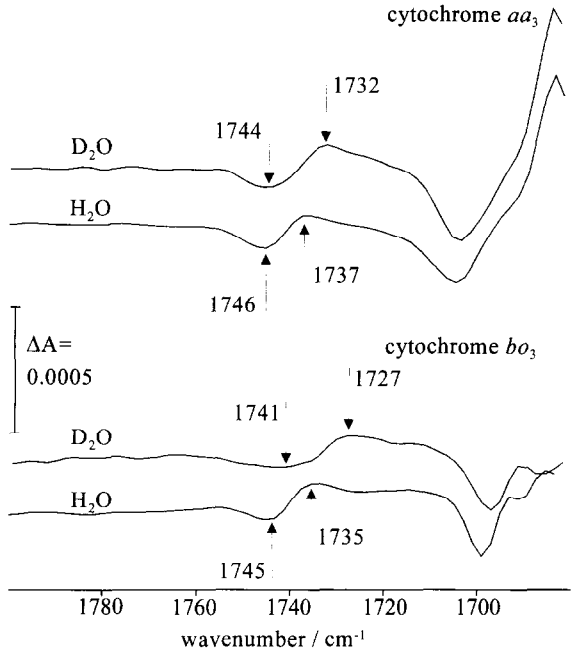

Fig. 4. Redox difference spectra between 1680 and 1800 cm^{-1} of cytochrome aa_3 of *Rhodobacter sphaeroides* (top) and of cytochrome bo_3 of *Escherichia coli* (bottom). The spectra were recorded from samples dissolved in buffer containing either H_2O or D_2O as solvents.

ance spectra is rather small. However, the caged reaction does not take place in the absence of an appropriate electron acceptor. As a further control experiment, redox FTIR difference spectra using horse heart cytochrome *c* as electron acceptor were recorded under the same conditions (data not shown). Test spectra measured with the caged electron technique using riboflavin were almost identical to those which have been reported by use of a spectroelectrochemical cell [13]. This comparison indicates little if any contribution of the caged compound and the resulting photolytic products to the infrared spectra.

Under these experimental conditions (compare with the experiment described in Fig. 2) the presence of the oxidase inhibitor KCN is not necessary, because the amount of dissolved oxygen is negligible due to the small sample volumes.

3.3. Interpretation of infrared redox difference spectra from haem-copper oxidases between 1000 and 1700 cm^{-1}

The redox FTIR difference spectra of cytochrome aa_3 of *R. sphaeroides* and cytochrome bo_3 of *E. coli* as depicted in Fig. 3 (left) exhibit different characteristic shapes, in which negative and positive peaks are indicative of the oxidized and reduced state of the proteins. The absorbance changes are rather small, at maximum 0.003 or 0.002 for the oxidases from *Rhodobacter* and *Escherichia*. The largest absorbance differences are found in the amide I region (1680–1620 cm^{-1}). In this region typical 'up-and-down' patterns can be seen with 1661 cm^{-1} (maximum)–1656 cm^{-1} (minimum)–1651 cm^{-1} (maximum)–1644 cm^{-1} (minimum) for the *Rhodobacter* and 1664 cm^{-1} (maximum)–1657 cm^{-1} (minimum)–1653 cm^{-1}(maximum)–1649 cm^{-1} (minimum) for the *Escherichia* oxidases. Amide I and water absorptions overlap spectrally in the region of 1680–1620 cm^{-1}. However, the band sharpness as well as the reproducibility of the band patterns indicate that the absorption of water did not contribute significantly to the obtained difference spectra. Correspondingly, within the amide II region, expanding from 1560 to 1520 cm^{-1}, maxima at 1549 and 1524 cm^{-1} (*Rhodobacter*) and 1537 and 1514 cm^{-1} (*Escherichia*) and an intense minimum at about 1564–1566 cm^{-1} are obvious. These changes in the amide regions could well correspond to conformational changes during the process of reduction, which has been recently discovered for the mitochondrial enzyme by circular dichroism spectroscopy [14]. However, the overall absorbance changes in the amide I region of 0.002–0.003 are very small compared to the total absorbance of about 1. Therefore, a slight change in the peptide backbone conformation involving 3 to 5 peptide bonds can be expected for the redox transient. This is consistent with the recently postulated 'histidine cycle' model of the reaction mechanism of cytochrome oxidase [7,15]. X-ray crystallographic analysis of oxidized and reduced forms of cytochrome oxidases most likely cannot demonstrate these small conformational changes at a resolution of 2.8 Å. This conclusion can be drawn in analogy to evidence reported for the $PQ \rightarrow P^+Q^-$ transition of photosynthetic reaction centres: light-minus-dark infrared spectra result in amide I absorbance changes of the same order, but X-ray difference Fourier analysis of the PQ and P^+Q^- states (3 Å resolution) could not disclose significant light-induced conformational changes [16,17].

The positive band at 1684 cm^{-1} and the strong negative band at 1685–1690 cm^{-1} are located in a region where haem groups absorb. Haems B and O of *Escherichia* and haems A from *Rhodobacter* are the essential cofactors of the oxidase and it is reasonable to assume contributions of the prosthetic groups to these peaks as reflecting structural changes accompanied by the redox transient. A number of additional peaks are in the spectral range below 1520 cm^{-1}, which could reflect changes in the global environment as well as of individual chemical bonds. Assignment of these signals into specific groups is probably important for the understanding of the mechanism of the oxidase. However, at present it is impossible to assort these bands. In fact, further information will be obtained by isotope-specific group labelling of the protein and introduction of site-specific changes by mutagenesis.

3.4. Infrared region between 1700–1800 cm^{-1}: involvement of carboxyl groups

The carbonyl absorption of side chains from glutamic and aspartic acids occurs in the region of 1680–1750 cm^{-1} (Fig. 4). In this range, the redox difference spectra of both cytochrome oxidases have a common feature, a negative peak at 1745–1746 cm^{-1} and a positive signal at 1735–1737 cm^{-1} (Fig. 3, left). After solvent isotope exchange from H_2O to D_2O these bands can be identified as resulting from carboxylic acid side chains: Binding of a deuteron instead of a proton increases the reduced masses μ of the oscillators and the signals are shifted slightly to lower frequencies, by 2–4 cm^{-1} for the negative peak and by 5–8 cm^{-1} for the positive peak (Fig. 4 (top: cytochrome aa_3 of *R. sphaeroides*, bottom: cytochrome bo_3 of *E. coli*)). Interestingly, this pattern is found in the cytochrome *c* as well as in the quinol oxidase.

It is reasonable to assume that the redox difference signals between 1735 and 1746 cm^{-1} from cytochrome aa_3 and cytochrome bo_3 originate from carboxylic acids. Their band shapes and the solvent isotope effects indicate that in both

enzymes these carboxylic acids undergo similar changes during photoreduction. The acidic amino acids are probably located at homologous positions in the proteins and may have a functional role in the reaction mechanism common to both types of haem-copper oxidases. Anyway, the presence of absorbance changes in the carbonyl region clearly demonstrates that at least one of the carboxyl groups, which are sensitive to the redox transition, must be in the protonated state in the oxidized form of the haem-copper oxidase.

The following scenarios can be suggested from the alterations of signals from carboxylic acids in the process of reduction. (1) The most simple interpretation would be the assumption of only one protonated carboxylic acid, which is in different orientations in oxidized and reduced state. This group would move into a more hydrophilic environment upon photoreduction. (2) More complicated explanations could involve more than one carboxylic acid in certain orientations, which are deprotonated and protonated during the reduction process. At present it is not possible to differentiate between possible mechanisms and to assess the exact role of carboxyl groups in proton translocation. Similarly, the protonation of carboxyl groups of the cytochrome *c* oxidase of *P. denitrificans* has been observed via a different experimental approach using a spectroelectrochemical cell [18].

The mechanism of proton translocation across the channel of the light-driven proton pump bacteriorhodopsin is under intense investigation and it is known to be rather complex in the small retinal protein [19–21]. Much structural information has been compiled from bacteriorhodopsin [22], but only a part of the functional groups contributing to the hydrogen-bonded network [21] of its proton channel have been resolved. A greater complexity may be expected from the much larger redox-driven proton pumps of the haem-copper oxidase type, which must provide two different intraprotein pathways for scalar and vectorial protons. Site-specific mutants in the respective protein regions composing the proton channel(s) as predicted from the 3D structural model [7,8], would be required to answer these questions. These experiments are in preparation.

Acknowledgements: The help of Dr. Benedikt Heßling in introducing M.L. to the FTIR technique is gratefully acknowledged. The work has been supported by the Deutsche Forschungsgemeinschaft (SFB 394, Projekt C6).

References

[1] Saraste, M. (1990) Q. Rev. Biophys. 23, 331–366.
[2] Saraste, M., Holm, L., Lemieux, L.J., Lübben, M. and Van der Oost, J. (1991) Biochem. Soc. Trans. 19, 608–612.
[3] Trumpower, B.L. and Gennis, R.B. (1994) Annu. Rev. Biochem. 63, 675–716.
[4] Lübben, M. (1995) Biochim. Biophys. Acta 1229, 1–22.
[5] Garcia-Horsman, J.A., Puustinen, A., Gennis, R. and Wikström, M. (1995) Biochemistry 34, 4428–4433.
[6] Fetter, J.R., Qian, J., Shapleigh, J., Thomas, J.W., Garcia-Horsman, A., Schmidt, E., Hosler, J., Babcock, G.T., Gennis, R.G. and Ferguson-Miller, S. (1995) Proc. Natl. Acad. Sci. USA 92, 1604–1608.
[7] Iwata, S., Ostermeier, C., Ludwig, B. and Michel, H. (1995) Nature 376, 660–669.
[8] Tsukihara, T., Aoyama, H., Yamashita, E., Tomizaki, T., Yamagushi, H., Shinzawa-Itoh, K., Nakashima, R., Yaono, R. and Yoshikawa, S. (1996) Science 272, 1136–1144.
[9] Warne, A., Wang, D.N. and Saraste, M. (1995) Eur. J. Biochem. 234, 443451.
[10] Salet, C., Land, E.J. and Santus, R. (1981) Photochem. Photobiol. 33, 753–755.
[11] Ahmad, I., Cusanovich, M.A. and Tollin, G. (1982) Biochemistry 21, 3122–3128.
[12] Tollin, G. (1995) J. Bioenerg. Biomembr. 27, 303–309.
[13] Moss, D., Nabedryk, E., Breton, J. and Mäntele, W. (1990) Eur. J. Biochem. 187, 565–572.
[14] Wittung, P. and Malmström, B. (1996) FEBS Lett. 388, 47–49.
[15] Morgan, J.E., Verkhovsky, M.I. and Wikström, M. (1994) J. Bioenerg. Biomembr. 26, 599–608.
[16] Gerwert, K., Hess, B., Michel, H. and Buchanan, S. (1988) FEBS Lett. 232, 303–307.
[17] Buchanan, S., Michel, H. and Gerwert, K. (1991) in: Reaction Centres of Photosynthetic Bacteria (Beyerle, M.E. ed.) Springer Series in Biophysics 6, pp. 75–85, Springer, New York.
[18] Hellwig, P., Rost, B., Kaiser, U., Ostermeier, C., Michel, H. and Mäntele, W. (1996) FEBS Lett. 385, 53–57.
[19] Oesterhelt, D., Tittor, J. and Bamberg, E. (1992) J. Bioenerg. Biomembr. 24, 181–191.
[20] Lanyi, J.K. and Varo, G. (1995) Isr. J. Chem. 35, 365–385.
[21] Le Coutre, J., Tittor, J., Oesterhelt, D. and Gerwert, K. (1995) Proc. Natl. Acad. Sci. USA 92, 4962–4966.
[22] Grigorieff, N., Ceska, T.A., Downing, K.H., Baldwin, J.M. and Henderson, R. (1996) J. Mol. Biol. 259, 393–421.
[23] Traber, R., Kramer, H.E.A. and Hemmerich, P. (1982) Biochemistry 21, 1687–1693.